

Spillover and Predictability of Volatility of 50 Major Cryptocurrencies: Evidence from a LASSO-Regularized Quantile VAR

September 27, 2025

Abstract

Previous studies examine spillover effects across the volatility of several cryptocurrencies in the mean or across quantiles without addressing the issue of high dimensionality. Using a large dataset of 50 cryptocurrencies, we employ a LASSO-regularized Quantile VAR framework and show that spillover effects differ across low, medium, and high volatility regimes, especially when evaluated dynamically over time, with sharp increases around tail events such as the war in Ukraine. Importantly, we demonstrate that the LASSO-QVAR model delivers statistically significant forecasting improvements over its univariate counterpart, underscoring the role of interconnectedness in enhancing volatility prediction across cryptocurrencies.

Keywords: Cryptocurrencies; Volatility; LASSO Quantile VAR; Spillovers; Forecasting

JEL: C32, C53, G10, G17

1 Introduction

The increasing interdependence of financial markets has accentuated the importance of understanding connectedness and spillover effects across assets. Cryptocurrencies, as a distinct and rapidly evolving asset class, exhibit unique dynamics driven by high volatility and interconnected behaviors.¹ Bitcoin, the first cryptocurrency, is based on blockchain technology and the genuine concept of mass collaboration. Launched in 2009, it has gradually inspired the construction of other cryptocurrencies, which vary in market size and significance, but

¹In this paper, we use the terms connectedness and spillover in close relation. While connectedness typically refers to the overall degree of interdependence within the system, spillover emphasizes the directional transmission of shocks across assets. We study both aspects: the overall degree of connectedness in the cryptocurrency market and the directional contributions of each cryptocurrency to and from others.

they are generally built around blockchain systems. The large and diverse universe of cryptocurrencies stands as a new (digital) asset class, with a market value exceeding 3.5 trillion USD around the end of 2024. It offers diversification opportunities for stock and bond investors (Bouri et al., 2017; Shahzad et al., 2019), especially during stressful periods, powered by the decentralization feature of most cryptocurrencies and their detachment from the expansion of balance sheets of US and European central banks (Kumar et al., 2022). Interestingly, the phenomenon of digitalization, accelerated by the pandemic’s aftermath during lockdowns and the shift to remote work, has led to increased attractiveness and demand for cryptoassets. Although the dominance of Bitcoin has been persistent over the past years, the importance of other cryptocurrencies such as Ethereum, Litecoin, XRP, Dogecoin, cannot be overstated by many practitioners and market participants.

Given the speculative nature of cryptocurrency and the lack of theoretical valuation model for cryptocurrency, the young and under-regulated cryptocurrency market exhibits a large price variability. The rapid development of cryptocurrencies continues to thrive on media attention (Philippas et al., 2019), sentiments and emotions (Ahn and Kim, 2021; Mokni et al., 2022; Anamika et al., 2023), and fear of missing out (FOMO) effect (Baur and Dimpfl, 2018).² Interestingly, the main commonalities that characterise the players in this new digital asset class are blockchain technology and the resulting decentralization from sovereign authorities, as well as exponential price appreciation and tremendous volatility, hype and fear-of-missing-out phenomena, and speculative activities, which all contribute to a different degree to heightened levels of market integration (Ji et al., 2019). Notably, cryptocurrencies are interconnected and one (large) cryptocurrency can affect other cryptocurrencies (Ji et al., 2019; Fasanya et al., 2021; Özdemir, 2022), especially under extreme events.

Traditional approaches to measuring connectedness, such as the Forecast Error Variance Decomposition (Pesaran and Shin, 1998; Diebold and Yilmaz, 2008, 2012, 2014), based on Vector AutoRegressive models (Lütkepohl, 2005), have proven effective in analyzing financial

²Aharon et al. (2022) highlight evidence of a causal spillover effect between Twitter-based uncertainty and the cryptocurrency markets.

networks. However, these methods often fail to capture the nonlinearities and heterogeneities inherent in financial systems, as they only focus on relationships involving conditional expectations. Recent advancements, including the Quantile Forecast Error Variance Decomposition (Ando et al., 2022), offer a more granular perspective by examining spillover effects across different quantiles of the variables' conditional distributions. This approach provides valuable insights into tail dependencies and extreme market conditions, which are particularly relevant in volatile markets like cryptocurrencies.

The volatility dynamics and cross-correlations of cryptocurrencies exhibit strong nonlinear feature (Chowdhury et al., 2023), which suggests the suitability of applying a spillover analysis across the various quantiles of the distribution of cryptocurrency volatility to reveal how various levels of volatility shocks are transmitted in the cryptocurrency markets.³ While the Quantile Forecast Error Variance Decomposition approach of Ando et al. (2022) has been used in the related literature to estimate tail dependencies and extreme market conditions, it is subject to the issue of high-dimensional quantile VARs when applied to a large set of cryptocurrencies. Interestingly, Yi et al. (2018) use a LASSO-VAR to estimate the spillover index in the mean; however, they overlook the spillover effects across high, medium and low volatility regimes.

Building on this foundation, the present study employs a LASSO-regularized Quantile Vector AutoRegressive framework (Caporin et al., 2023) to estimate connectedness and spillovers across a network of 50 cryptocurrencies. The LASSO regularization technique (Tibshirani, 1996) enhances the model's predictive accuracy and sparsity, addressing the curse of dimensionality.

Accordingly, our analysis takes a deeper and more comprehensive view on the volatility interdependence in the cryptocurrency markets by applying a novel approach that addresses the shortcomings of quantile-VAR spillover literature faced when dealing with a large set of cryptocurrencies. By employing a LASSO-Quantile VAR for estimating a high-dimensional

³Liu et al. (2025) argue that the fast expansion of the cryptocurrency market has induced substantial price volatility, causing asymmetry and extreme tail-dependency.

quantile VAR, it advances the related literature that uses the LASSO-VAR (Yi et al., 2018) and the one that applies quantile-based approaches of connectedness (Bouri et al., 2021; Karim et al., 2022; Mensi et al., 2023). This allows us to capture the dynamics and network of volatility connectedness across a large number of cryptocurrencies in a granulated way, revealing a profounder understanding of how volatility shocks propagates among various volatility regimes. Typically, large volatility shocks tend to be transmitted more easily that small volatility shocks, leading to more intensification in the spillover index at the high volatility regime compared to the low volatility regime.

We further enrich our analysis by analysing the network following the Factor-Adjusted Network Estimation and Forecasting for High-Dimensional Time Series (FNETS) method recently proposed by Barigozzi et al. (2023), which accounts for the effects of potential common factors. Furthermore, The FNETS method estimates the network of high-dimensional cryptocurrencies although cryptocurrencies are subject to serial correlation and cross-sectional dependencies.

Taken together, our analysis is particularly new in the literature that focuses on the highly volatile and speculative market of cryptocurrencies. It should help various participants in the cryptocurrency market in making more refined and granulated decisions, possibly guiding enhanced investment and risk inferences in a new digital asset class that continues to draw attention and regulatory oversight from policymakers and central banks.

The rest of the paper goes as follows. Section 2 reviews the related literature in the area of cryptocurrencies, especially the volatility spillover analysis. Section 3 presents the LASSO-regularized Quantile VAR framework of spillover and the FNETS method. Section 4 describes the dataset and empirical setup. Section 5 presents the empirical findings. Section 6 concludes the paper.

2 Related literature

Following the emergence of cryptocurrencies as a separate asset class, attractive to investment and trading strategies given its somewhat independence from sovereign authorities despite its large volatility, a growing literature considers the interactions across major cryptocurrencies for the sake of understanding the complexity of such interactions and making insightful inferences regarding portfolio and risk management. Previous studies on the interconnection and dependence among various cryptocurrencies demonstrate that Bitcoin is typically the most influential one for the dynamics of co-jumps (Zhang et al., 2023), co-bubbling (Bouri et al., 2019b), and market contagion (Antonakakis et al., 2019). Furthermore, herding behaviour is found to be significant among participants in the cryptocurrency markets (Bouri et al., 2019a; Gurdgiev and O’Loughlin, 2020; Yousaf and Yarovaya, 2022).

Notably, evidence of significant transmission of volatility across various cryptocurrencies is often found, **underling** the influential role of large cryptocurrencies such as Bitcoin and Ethereum (Yi et al., 2018; Ji et al., 2019; Fasanya et al., 2021), and evidence of instability around crisis periods and event shocks such as the COVID-19 outbreak; see, among others, Maghyereh and Ziadat (2024).

Yi et al. (2018) estimate the spillover index across several cryptocurrencies in the mean, although they integrate the LASSO technique in the spillover analysis to address the issue of a high-dimensional VAR. Their results **highlights the significant role played** large-cap cryptocurrencies in the system of volatility spillovers. Ji et al. (2019) study the VAR-based spillover effects in volatility in the system of six major cryptocurrencies over the period August 2015—February 2018, revealing the key role played by Bitcoin without ignoring the importance of other large cryptocurrencies such as Litecoin. Xu et al. (2021) examine the tail-risk dependencies across 23 cryptocurrencies by employing a TENET approach. They underline evidence of significant risk spillover effect that has been on the rise.

The relevance of extreme shocks and events such as the pandemic and the war in Ukraine on the dynamics of cryptocurrencies has been the subject of previous studies. Accordingly,

the interactions among large cryptocurrencies are noticed, indicating a spike in the level of spillover effects around these crisis periods, and showing evidence that large cryptocurrencies such as Bitcoin and Ethereum are key to the system of spillovers. In this regard, Karim et al. (2022) find significant risk spillovers across conventional and non-conventional cryptocurrencies (e.g., DeFi and NFTs) during crisis periods using a quantile approach of spillovers. Using a spillover index within a VAR framework, Kumar et al. (2023) show a heightened level of spillovers just before the war in Ukraine. Chowdhury et al. (2023) consider the efficiency of various cryptocurrencies using an asymmetric multifractal approach. They show the significant effect of the pandemic on the efficiency of the cryptocurrency markets and find that the volatility dynamics of cryptocurrencies exhibit strong nonlinear **feature** in their cross-correlations. Koutmos (2018) applies the spillover approach of Diebold and Yilmaz (2008, 2012, 2014) and shows that the transmission of return and volatility shocks across 18 major cryptocurrencies is on the rise, reflecting a contagion risk. Bitcoin is a major contributor to this contagion risk, which intensifies under news shocks related to cryptocurrencies. Katsiampa et al. (2019) apply a multivariate GARCH model and show that the largest cryptocurrency, Bitcoin, is bidirectionally related with Ethereum and Litecoin in terms of both return and volatility shocks. Kumar and Anandarao (2019) study the interlinkages of volatility in the cryptocurrency markets using GARCH and wavelet techniques, and reveal evidence of a moderate volatility spillover effect, which is shaped by the market of Bitcoin and various exogenous shocks. Liu and Serletis (2019) show, based on a multivariate GARCH-in-mean model, that the volatility of Bitcoin, Ethereum, and Litecoin **are** somewhat interrelated. Notably, the volatility shocks in Litecoin can heighten the volatility of Ethereum, but they exert no influence on Bitcoin volatility. Fasanya et al. (2021) apply the spillover approach of Diebold and Yilmaz (2008, 2012, 2014) on various cryptocurrencies and report evidence of significant return and volatility spillovers, with Bitcoin and Ethereum playing the roles of transmitters of shocks, suggesting an increasing integration and contagion risk across major cryptocurrencies, which **ultimately** investment decisions and portfolio management. Özdemir

(2022) studies the volatility spillovers eight large cryptocurrencies (Bitcoin, Ethereum, Stellar, Ripple, Tether, Cardano, Litecoin, and Eos) over the period November 2019—January 2021, covering the pandemic. Applying GARCH and wavelet based methods, the author finds that large cryptocurrencies, namely Bitcoin, Ethereum, and Litecoin, are very volatile and interrelated. Furthermore, their downside risk is much larger than that of Chinese and US equity indices. Liu and Serletis (2024) employ a GARCH-copula model and find evidence of tail-dependence between financial and cryptocurrency markets. Furthermore, they find a lower tail-dependence across Bitcoin, Ethereum, and Litecoin.

On a related front, Maghyreh and Ziadat (2024) report evidence of significant tail risk spillovers across six leading cryptocurrencies, which seem to spike around crisis periods. They also show the important role played by investor sentiment, macroeconomic conditions, and economic uncertainty in affecting the spillovers. Liu et al. (2025) propose a Mean-ES risk optimization framework and capture asymmetry and tail-dependence in the cryptocurrency markets, while providing implications for the optimized portfolio and risk management.

The above-mentioned literature has been useful to understand the volatility linkages among major cryptocurrencies. It relies on standard approaches **that** built on GARCH-based modelling and wavelet coherence, and many of the related studies either employ VAR-based measures of connectedness that capture the evolution of the degree of volatility connectedness during normal and crisis periods or the quantile-VAR measures without addressing high-dimensionality issues. Our current paper seeks to address these issues and accordingly contributes to the related literature on cryptocurrency volatility connectedness by applying the LASSO-regularized Quantile VAR framework (Caporin et al., 2023) to estimate connectedness and spillovers across a network of 50 cryptocurrencies. The LASSO regularization technique (Tibshirani, 1996) enhances the model’s predictive accuracy and sparsity, addressing the curse of dimensionality.

3 Connectedness in high-dimensional settings

Let $p_{j,t}^{\text{high}}$ and $p_{j,t}^{\text{low}}$ be, respectively, the maximum and the minimum log-prices of cryptocurrency j on day t . Following Barigozzi et al. (2023) and Brownlees and Gallo (2009), we estimate the log-volatility of cryptocurrency j on day t as follows:

$$y_{j,t} = \log \left[0.361 \left(p_{j,t}^{\text{high}} - p_{j,t}^{\text{low}} \right)^2 \right]. \quad (1)$$

We then define the $N \times 1$ vector $\mathbf{y}_t = [y_{1,t} \cdots y_{N,t}]'$, for $t = 1, \dots, T$. We study the propagation of the spillovers within the network of the $y_{1,t} \cdots y_{N,t}$ variables using a generalization of the Quantile Forecast Error Variance Decomposition (QFEVD) introduced by Ando et al. (2022), that we describe below.

We start from the reference methodology: the Forecast Error Variance Decomposition (FEVD), that is based on the following Vector AutoRegressive (VAR) model:

$$\mathbf{y}_t = \boldsymbol{\alpha} + \sum_{k=1}^p \boldsymbol{\Phi}_k \mathbf{y}_{t-k} + \mathbf{u}_t, \quad (2)$$

where $\boldsymbol{\Phi}_k$ is an $N \times N$ parameter matrix, $\boldsymbol{\alpha} = [\alpha_1 \cdots \alpha_N]'$ is the $N \times 1$ vector of intercepts, and $\mathbf{u}_t \sim \mathcal{N}(\mathbf{0}, \boldsymbol{\Sigma})$ is the error term (Pesaran and Shin, 1998; Lütkepohl, 2005; Diebold and Yilmaz, 2008, 2012, 2014).

Given the parameters of the VAR model in Equation (2), we obtain the $N \times N$ FEVD matrix for a given forecast horizon h . Following Pesaran and Shin (1998), we focus on the generalized impulse response function, as it provides estimates that do not depend on the ordering of the $y_{1,t} \cdots y_{N,t}$ variables in \mathbf{y}_t . We then define entry (i, j) of the FEVD matrix as:

$$\theta_{i,j}(h) = \frac{\sigma_{jj}^{-1} \sum_{l=0}^h (\mathbf{e}_i' \boldsymbol{\Gamma}_l \boldsymbol{\Sigma} \mathbf{e}_j)^2}{\sum_{l=0}^h (\mathbf{e}_i' \boldsymbol{\Gamma}_l \boldsymbol{\Sigma} \boldsymbol{\Gamma}_l' \mathbf{e}_i)}, \quad (3)$$

where $\text{diag}(\boldsymbol{\Sigma}) = [\sigma_{11} \cdots \sigma_{NN}]$, $\boldsymbol{\Gamma}_l$ is a function $\boldsymbol{\Phi}_k$ derived through an infinite moving average representation of the VAR model in Equation (2), and \mathbf{e}_i is an $N \times 1$ selection vector with

zero elements, except the i -th one, which is equal to one.

$\theta_{i,j}(h)$ is the proportion of the h -step ahead forecast error variance of variable i which is accounted for by the innovations in variable j . However, the sum of $\theta_{i,1}(h), \dots, \theta_{i,N}(h)$ is not necessarily equal to one, for each $i = 1, \dots, N$. We then normalize the entries of the FEVD matrix:

$$\tilde{\theta}_{i,j}(h) = \frac{\theta_{i,j}(h)}{\sum_{j=1}^N \theta_{i,j}(h)} \cdot 100 \quad (4)$$

for $i = 1, \dots, N$; see, among others, Gross and Siklos (2019).

We also estimate the contribution from and to others of each node within the overall network. Specifically, following Diebold and Yilmaz (2008, 2012, 2014), we define the total directional connectedness to others from variable j :

$$\tilde{\theta}_{\bullet \leftarrow j}(h) = \frac{1}{N-1} \sum_{\substack{i=1 \\ i \neq j}}^N \tilde{\theta}_{i,j}(h) \quad (5)$$

and the total directional connectedness from others to variable i :

$$\tilde{\theta}_{i \leftarrow \bullet}(h) = \frac{1}{N-1} \sum_{\substack{j=1 \\ j \neq i}}^N \tilde{\theta}_{i,j}(h). \quad (6)$$

From the difference $\tilde{\theta}_{\bullet \leftarrow j}(h) - \tilde{\theta}_{j \leftarrow \bullet}(h)$, it is possible to quantify the net contribution of node j . At a global level, we also define the total spillover index:

$$\tilde{\theta}(h) = \frac{1}{N} \sum_{\substack{i=1 \\ i \neq j}}^N \sum_{j=1}^N \tilde{\theta}_{i,j}(h). \quad (7)$$

The FEVD methodology depends on the parameters of the VAR model given in Equation (2), which relate the lagged values of $y_{1,t}, \dots, y_{N,t}$ with their current expectations. However, such relationships could change along the conditional distributions of the $y_{1,t}, \dots, y_{N,t}$ variables. Inspired by this idea, Ando et al. (2022) extended the FEVD method to the quantile

framework, introducing the QFEVD model, which builds on the Quantile VAR (QVAR) model. Given $\tau \in (0, 1)$, let $Q_\tau(y_{i,t}|\mathcal{I}_{t-1})$ be the τ -th quantile of $y_{i,t}$ conditional on the information set available at time $t - 1$ with the following specification:

$$Q_\tau(y_{i,t}|\mathcal{F}_{t-1}) = \alpha_{i,\tau} + \sum_{k=1}^p \Phi_{k,\tau}^{(i)} \mathbf{y}_{t-k}. \quad (8)$$

Equation (8) is the i -th equation of the QVAR system, with $i = 1, \dots, N$, and is estimated by employing the quantile regression model introduced by Koenker and Bassett (1978). We use $\Phi_{k,\tau}^{(i)}$ as the i -th row of the $N \times N$ matrix $\Phi_{k,\tau}$, with $i = 1, \dots, N$ and $k = 1, \dots, p$. Note that, in contrast to Φ_k , $\Phi_{k,\tau}$ depends on the quantile level τ . By replacing Φ_k with $\Phi_{k,\tau}$, it is possible to obtain the quantile counterpart of Γ_l , denoted as $\Gamma_{l,\tau}$. Furthermore, we define the covariance matrix of the QVAR error terms as Σ_τ . As a result, entry (i, j) of the QFEVD matrix has the following form:

$$\theta_{i,j}(h, \tau) = \frac{\sigma_{jj,\tau}^{-1} \sum_{l=0}^h (\mathbf{e}_i' \Gamma_{l,\tau} \Sigma_\tau \mathbf{e}_j)^2}{\sum_{l=0}^h (\mathbf{e}_i' \Gamma_{l,\tau} \Sigma_\tau \Gamma_{l,\tau}' \mathbf{e}_i)}, \quad (9)$$

where $\text{diag}(\Sigma_\tau) = [\sigma_{11,\tau} \cdots \sigma_{NN,\tau}]$.

By replacing $\theta_{i,j}(h)$ with $\theta_{i,j}(h, \tau)$ in Equations (4)–(7), it is possible to compute the quantile-specific indicators $\tilde{\theta}_{\bullet \leftarrow j}(h, \tau)$, $\tilde{\theta}_{i \leftarrow \bullet}(h, \tau)$, and $\tilde{\theta}(h, \tau)$, respectively.

In a recent study, Caporin et al. (2023) noticed that the QFEVD spillover index is affected by distortions that become more relevant at extreme quantile levels (i.e. when τ approaches to either zero or one). Interestingly, the magnitude of such distortions is quite symmetric in the left and right tails, and the resulting QFEVD spillover index exhibits a kind of U shape (Caporin et al., 2023). Building on an extensive simulation analysis, Caporin et al. (2023) showed that such distortions could be significantly reduced by implementing regularization techniques, such as the Least Absolute Shrinkage and Selection Operator (LASSO) introduced by Tibshirani (1996). In particular, Caporin et al. (2023) employed the ℓ_1 -penalized quantile regression estimator (Koenker, 2005; Belloni and Chernozhukov, 2011)

to estimate the QVAR parameters, by minimizing, for each equation i ($i = 1, \dots, N$), the following loss function:

$$\frac{1}{T-p} \sum_{t=p+1}^T \rho_{\tau} \left(y_{i,t} - \alpha_{i,\tau} - \sum_{k=1}^p \Phi_{k,\tau}^{(i)} \mathbf{y}_{t-k} \right) + \lambda^{(i)} \frac{\sqrt{\tau(1-\tau)}}{T-p} \sum_{k=1}^p \sum_{j=1}^N \hat{\sigma}_j \left| \phi_{k,\tau,j}^{(i)} \right|,$$

where $\phi_{k,\tau,j}^{(i)}$ is the j -th entry of $\Phi_{k,\tau}^{(i)}$, $\hat{\sigma}_j$ is the sample standard deviation of $y_{j,t}$, $\lambda^{(i)} \geq 0$ is a tuning parameter, $\rho_{\tau}(u) = u(\tau - \mathbb{I}_{\{u < 0\}})$ is the asymmetric loss function of quantile regression (Koenker and Bassett, 1978), and $\mathbb{I}_{\{\cdot\}}$ is an indicator function which is equal to one if the condition in $\{\cdot\}$ is true, and equal to zero otherwise.

Note that $\lambda^{(i)}$ controls the sparsity of the solutions: the greater $\lambda^{(i)}$, the greater the number of parameters in the i -th QVAR equation that approach zero. Following Caporin et al. (2023), we adopt the method proposed by Belloni and Chernozhukov (2011) to select the optimal value of $\lambda^{(i)}$.

We adopt the LASSO-regularized QFEVD model (Ando et al., 2022; Caporin et al., 2023) to estimate the contribution to and from others and the net contribution of each cryptocurrency in our dataset, as well as the overall spillover index for different quantile levels. Furthermore, we also assess the predictive accuracy of the underlying LASSO-regularized QVAR model. Let $\hat{\alpha}_{i,\tau}$ and $\hat{\Phi}_{k,\tau}^{(i)}$ be the LASSO-regularized estimates of $\alpha_{i,\tau}$ and $\Phi_{k,\tau}^{(i)}$, respectively. We stress the fact that such coefficients are obtained from response variables observed at time t and regressors observed at times $t-1, \dots, t-k$, consistent to the specification given in Equation (8). Building on such estimates and on the data available until time t , we can forecast the τ -th quantile of each variable i (with $i = 1, \dots, N$) at time $t+1$ as:

$$\hat{Q}_{\tau}(y_{i,t+1} | \mathcal{F}_t) = \hat{\alpha}_{i,\tau} + \sum_{k=0}^p \hat{\Phi}_{k,\tau}^{(i)} \mathbf{y}_{t-k}. \quad (10)$$

On the basis of the rolling window scheme described in Section 4, we iteratively contrast the forecast $\hat{Q}_{\tau}(y_{i,t+1} | \mathcal{F}_t)$ with the out-of-sample realization $y_{i,t+1}$ and, following Bonaccolto

et al. (2018), compute the following loss function:

$$\mathcal{L}_{i,t+1,\tau} = \left[\tau - I_{\{y_{i,t+1} - \widehat{Q}_\tau(y_{i,t+1}|\mathcal{F}_t) < 0\}} \right] \left[y_{i,t+1} - \widehat{Q}_\tau(y_{i,t+1}|\mathcal{F}_t) \right], \quad (11)$$

where $I_{\{\cdot\}}$ is an indicator function which takes the value of one if the condition in $\{\cdot\}$ is true, and the value of zero otherwise.

In addition to the regularized LASSO-QFEVD model, for comparison purposes, we also estimate the network of the $y_{1,t} \cdots y_{N,t}$ variables using another recent approach: the FNETS method introduced by Barigozzi et al. (2023). By doing so, we also assess the effects of potential common factors. The FNETS method allows us to estimate networks of high-dimensional time series potentially affected by strong serial and cross-sectional dependencies. It builds on a factor-adjusted VAR model in which it is possible to separate common factor-driven dynamics from sparse and idiosyncratic dependencies. More precisely, we decompose \mathbf{y}_t as:

$$\mathbf{y}_t = \mathbf{f}_t + \boldsymbol{\xi}_t, \quad (12)$$

where \mathbf{f}_t and $\boldsymbol{\xi}_t$ are, respectively, the latent factor-driven and the idiosyncratic components.

Barigozzi et al. (2023) employed the most general approach to high-dimensional time series factor modeling: the generalized dynamic factor model introduced by Forni et al. (2000), in which factors have both contemporaneous and lagged effects on $y_{1,t} \cdots y_{N,t}$, being then dynamic. The idiosyncratic component $\boldsymbol{\xi}_t$ is modeled with a sparse VAR process, which captures weak residual dependencies after removing the dominant co-movements due to common factors. In particular, the idiosyncratic VAR parameters are estimated using an ℓ_1 -regularized Yule-Walker estimator, and represent the Granger's (1969) causal links of a directed network.

Barigozzi et al. (2023) showed that, under mild conditions that also allow for heavy-tailed distributions, FNETS provides a consistent network estimation in simulations and real-world applications, even if the number of variables and the sample size diverge.

4 Data and empirical setup

This study employs a large set of cryptocurrency data, which consists of the closing price of 50 large cryptocurrencies against the USD, collected from CoinMarketCap as of May 2024 according to data availability.⁴ Selected out of a larger pool of more than 100 large cryptocurrencies, the 50 cryptocurrencies were filtered to ensure a price data spanning a minimum sample period from August 8, 2015 to May 5, 2024, which allows to study calm and turbulent periods, covering the pandemic, the war in Ukraine, the 2017 and March 2020-November 2021 crypto bull runs, the major correction of 2018, and the FTX collapse of 2022. Table A1 given in Appendix A provides details on the 50 cryptocurrencies examined, including name, symbol, daily trading volume, and market cap.

Following Caporin et al. (2023), we estimate the LASSO-regularized QFEVD model in our empirical analysis by setting $p = 1$ and $h = 10$. We assess the predictive accuracy of the underlying LASSO-regularized QVAR model building on a rolling window scheme with window size of 500 daily observations and step of one day ahead. Specifically, we iteratively divide our overall dataset in which we have $T = 2,129$ daily observations for each time series into 1,629 equally sized subsamples, each of which spans a time interval of 500 days. As a result, the first subsample includes the log-volatility time series from the first to the 500-th day. The second subsample is obtained by removing the oldest observations and including the ones of the 501-th day. This procedure continues until the 1,629 subsample, that spans the time period from the 1,629-th to the 2,128 day. For each subsample ending at time t , we iteratively contrast the in-sample estimates obtained at time t with the out-of-sample observations available at time $t + 1$, and compute the $\mathcal{L}_{i,t+1,\tau}$ loss function given in Equation (11), for $i = 1, \dots, N = 50$. We denote the average loss for each time series i and each quantile level τ as:

$$\bar{\mathcal{L}}_{i,\tau} = \frac{1}{1629} \sum_{t=500}^{2128} \mathcal{L}_{i,t+1,\tau}. \quad (13)$$

⁴Data are available at <https://coinmarketcap.com>.

We use as benchmark a simple univariate quantile AutoRegressive (QAR) model with the following specification:

$$Q_\tau(y_{i,t}|\mathcal{F}_{t-1}) = \alpha_{i,\tau} + \phi_{1,\tau}^{(i)}y_{i,t-1} \quad (14)$$

where the quantile of $y_{i,t}$ only depends on $y_{i,t-1}$ and, thus, is not affected by the lagged values of the other variables in \mathbf{y}_t , for $i = 1, \dots, 50$.

Similar to the procedure described above for the LASSO-regularized QVAR model, we also compute the loss function in (11) using the coefficients obtained from the estimation of the QAR model in Equation (14). We denote the average loss provided by the univariate QAR model as $\tilde{\mathcal{L}}_{i,\tau}$. We then compare the predictive accuracy of the two competing models using the Diebold and Mariano's (2002) test, by specifying the alternative hypothesis that QAR is less accurate than the regularized-LASSO QVAR model.

5 Empirical findings

We begin by examining the relevance of each variable in \mathbf{y}_t as implied by the LASSO-regularized QFEVD model across different quantile levels. We display in Figure 1 the contribution to others ($\tilde{\theta}_{\bullet \leftarrow j}(10, \tau)$, top panel), the contribution from others ($\tilde{\theta}_{j \leftarrow \bullet}(10, \tau)$, middle panel), and the net contribution ($\tilde{\theta}_{\bullet \leftarrow j}(10, \tau) - \tilde{\theta}_{j \leftarrow \bullet}(10, \tau)$, bottom panel) of each variable j along the quantile levels 0.1, 0.5, and 0.9. The values of $\tilde{\theta}_{\bullet \leftarrow j}(10, \tau)$ are substantially different for the $N = 50$ variables in \mathbf{y}_t . The largest contributions to others are observed for NEO (average contribution of 2.6 along the three quantile levels), ETH (average contribution of 2.6), and QTUM (average contribution of 2.5). In contrast, USDT, PRO, and NMR have the lowest contributions of, respectively, 0.5, 0.6, and 0.8 on average. For all cryptocurrencies, the values of $\tilde{\theta}_{\bullet \leftarrow j}(10, \tau)$ are substantially stable across the quantile levels 0.1, 0.5, and 0.9. The contributions from others exhibit a more homogeneous distribution across the $N = 50$ analysed cryptocurrencies (the average value of $\tilde{\theta}_{j \leftarrow \bullet}(10, \tau)$ is equal to

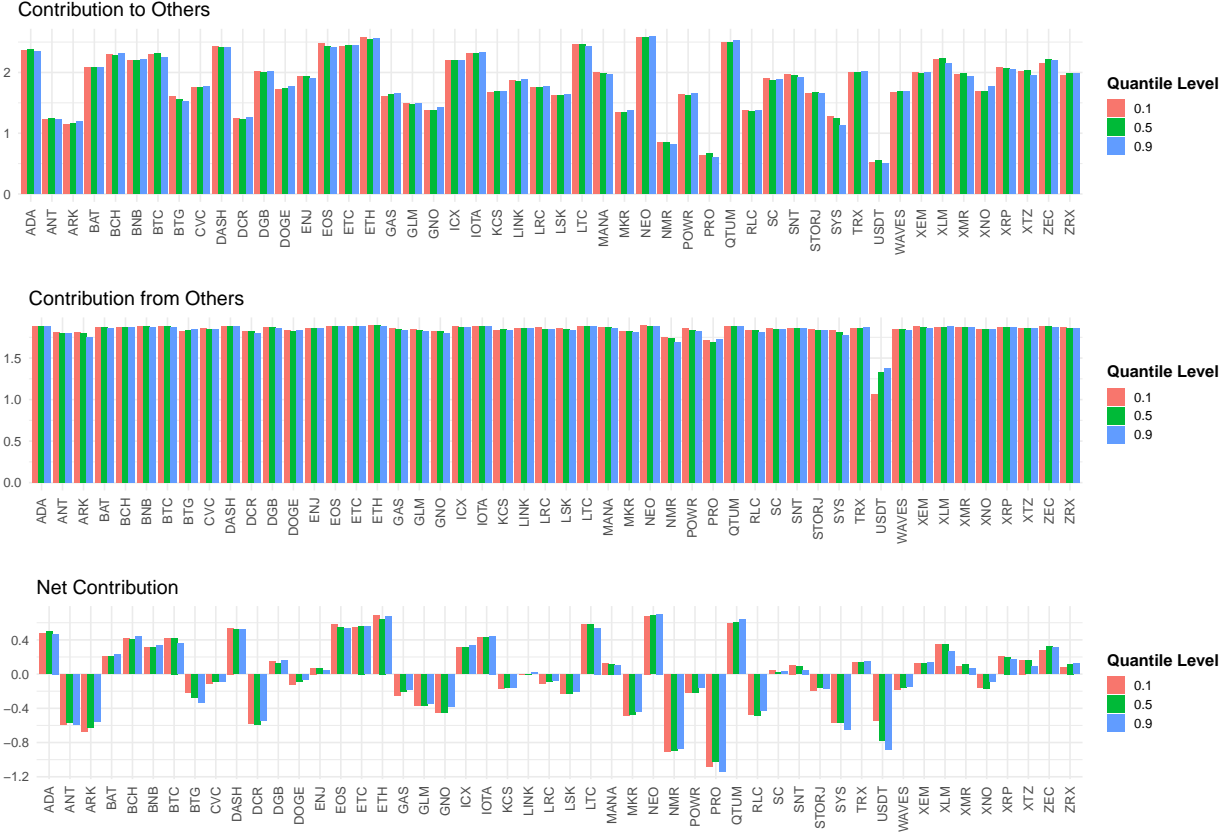


Figure (1) Contribution to and from others, and net contribution of each cryptocurrency resulting from the LASSO-regularized QFEVD estimated at the quantile levels 0.1, 0.5, and 0.9 on the full-sample data.

1.8). USDT shows a greater distance from the other cryptocurrencies, with a lower contribution from others equal to 1.26, on average. 28 cryptocurrencies have, on average, positive net contributions. Among them, we mention ETH, NEO, and QTUM, for which we observe the largest $\tilde{\theta}_{\bullet \leftarrow j}(10, \tau) - \tilde{\theta}_{j \leftarrow \bullet}(10, \tau)$ values of 0.7, 0.7, and 0.6, on average. In contrast, PRO and NMR have the largest negative net impact (below -0.8). These results suggest that systemic influence may extend beyond Bitcoin and Ethereum, with certain medium-sized cryptocurrencies also playing a significant role. Hence, risk monitoring focused solely on the two dominant cryptocurrencies could overlook relevant contagion channels.

After analyzing the contributions of the individual variables, we now aggregate the information into the overall spillover index. Figure 2 reports the values of $\tilde{\theta}(10, \tau)$ for quantile levels τ ranging from 0.1 to 0.9. Starting from values of around 92.1 at τ equal to 0.1 and 0.2,

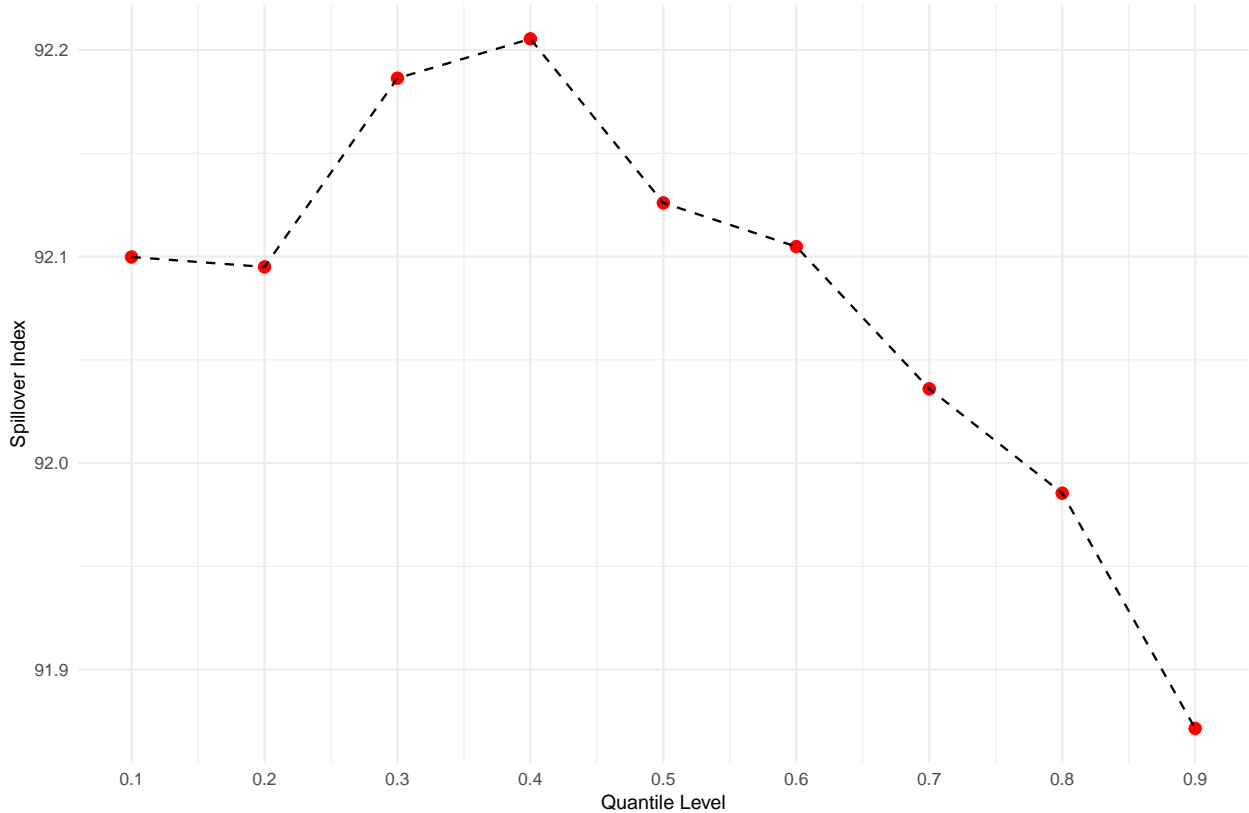


Figure (2) Spillover index as a function of the quantile levels from 0.1 to 0.9 resulting from the LASSO-regularized QFEVD estimated on the full-sample data.

the spillover index has an increasing trend up to $\tau = 0.4$, where it takes its maximum value of 92.2. Subsequently, there is a decreasing trend up to $\tau = 0.9$, where we observe the minimum of $\tilde{\theta}(10, \tau)$, equal to 91.9. Therefore, it takes values in the narrow interval $[91.9, 92.2]$, with a range of 0.3, having then a quite stable trend along the quantile levels from 0.1 to 0.9. While at first glance the numerical differences may appear negligible, this stability is itself an important finding. In contrast to traditional financial markets, where connectedness often intensifies in the tails, the cryptocurrency market exhibits consistently high integration across volatility conditions. This suggests that interdependence is a structural feature of the system rather than a regime-dependent phenomenon. For market participants, this implies facing a persistently high level of interconnectedness that does not vanish in calmer regimes. From a risk management perspective, portfolio diversification within the cryptocurrency

space may therefore be less effective than commonly assumed, as shocks propagate widely and consistently across assets regardless of volatility conditions.

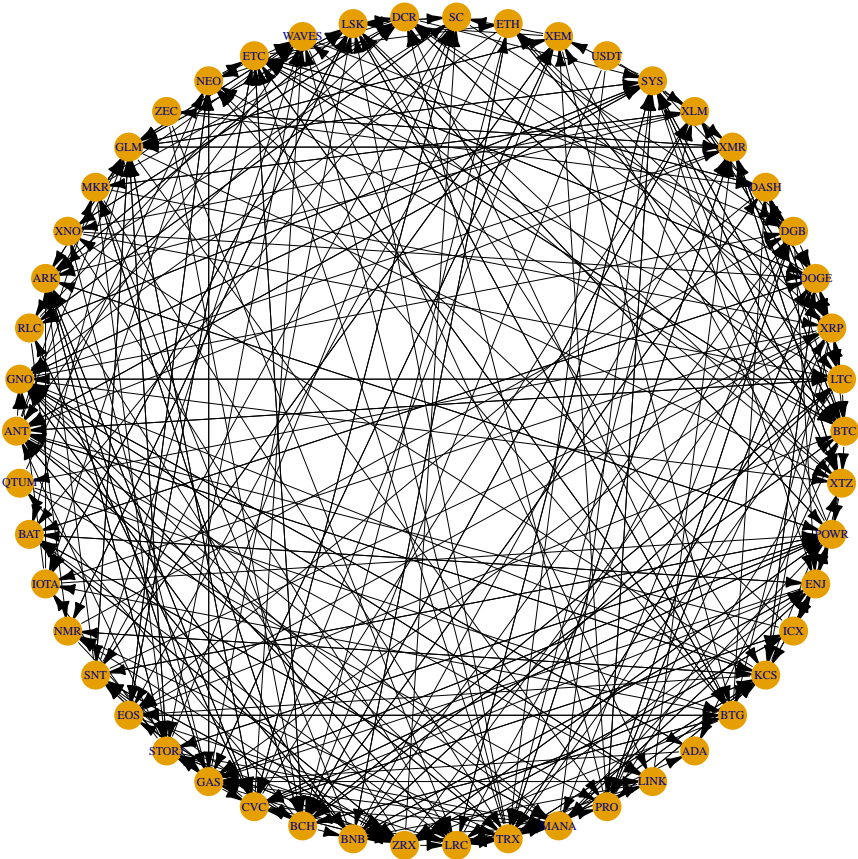


Figure (3) Granger's (1969) causality network estimated on the links of the idiosyncratic components of the log-volatility time series with the FNETS method.

To complement these spillover-based findings, we also employ the FNETS methodology (Barigozzi et al., 2023), which decomposes the dynamics into common factor-driven and idiosyncratic components. While the LASSO-QVAR captures directional spillovers at different quantile levels, thereby reflecting heterogeneous volatility regimes, FNETS isolates the

network of causal linkages among the idiosyncratic parts once common factors have been filtered out. Figure 3 reports the resulting Granger’s (1969) causality network based on the idiosyncratic components of log-volatility. The network reveals a relatively tight-knit structure, with several non-Bitcoin/Ethereum assets playing an influential role. Albeit derived from different perspectives, the two approaches, taken together, underscore the persistent interconnectedness of cryptocurrency volatility.

The results discussed so far are based on full-sample estimates. However, it is important to note that these full-sample estimates aggregate information over a long time interval, covering both tranquil and turbulent periods. Such aggregation inevitably smooths out quantile-specific differences and conceals the dynamics that characterize episodes of market stress. Moreover, given a long full-sample size ($T = 2,129$) and a fixed cross-sectional dimension ($N = 50$), the role of LASSO regularization is less critical in the full-sample estimation, as the curse of dimensionality is not particularly severe in this setting. Therefore, we also perform a rolling-window analysis, which reveals how the spillover index evolves over time and highlights substantial cross-quantile differences during crises.

We display in Figure 4 the trend of the spillover index $\tilde{\theta}(10, \tau)$ over time, setting τ equal to 0.1, 0.5, and 0.9. It significantly increases from the beginning of 2022, reaches its maximum value on September 2022, and continues to remain high until the end of 2023. In most subsamples determined with the rolling window scheme (57% of the 1,629 subsamples), it takes higher values at $\tau = 0.9$, whereas the lowest values are generally observed at $\tau = 0.1$. Importantly, the distance between quantile-specific indices is not stable over time: while differences are modest in tranquil periods, they widen significantly during episodes of stress, such as the COVID-19 pandemic and the war in Ukraine. This temporal pattern underscores that the cryptocurrency market becomes particularly vulnerable during episodes of heightened uncertainty. The increase in spillovers following major stress events suggests that crises act as amplifiers of systemic risk by strengthening the channels of shock transmission across assets. For policymakers and market participants alike, this implies that monitor-

ing connectedness dynamics in real time can provide early signals of fragility and potential contagion, helping to anticipate phases of market-wide instability.

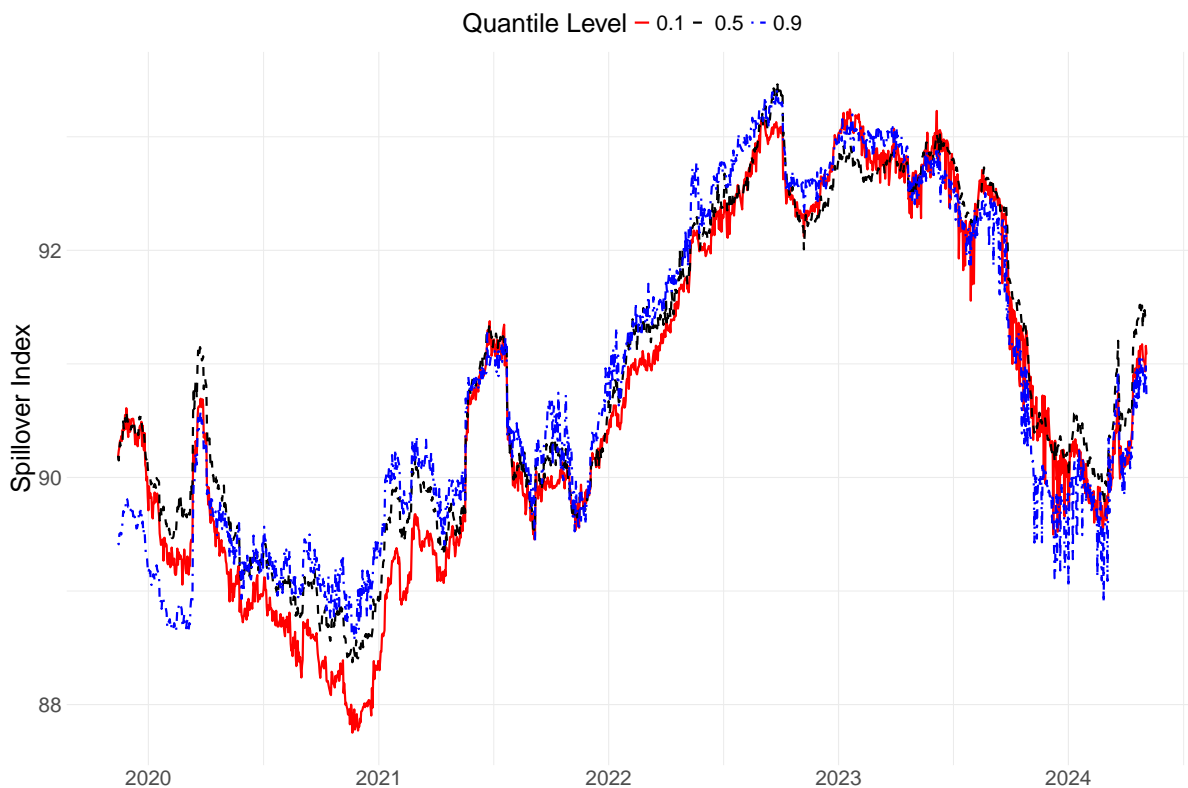


Figure (4) Spillover index $\tilde{\theta}(10, \tau)$ resulting from the estimation of the LASSO-regularized QFEVD model, by employing the rolling window scheme with subsamples of 500 daily observations and step of one days ahead.

Building on the estimates obtained from the rolling window scheme, we now evaluate the predictive accuracy of the LASSO-regularized QVAR model, comparing it with the univariate QAR specification on the basis of the Diebold and Mariano's (2002) test. We show the results of this test in Figure 5. Here, we display the $(\tilde{\mathcal{L}}_{i,\tau} - \bar{\mathcal{L}}_{i,\tau})$ differences, for $i = 1, \dots, 50$ and τ equal to 0.1 (top panel), 0.5 (middle panel), and 0.9 (bottom panel). We remind the reader that positive values of $(\tilde{\mathcal{L}}_{i,\tau} - \bar{\mathcal{L}}_{i,\tau})$ are due, on average, to larger losses resulting from the univariate QAR specification and, thus, to a better performance of the QVAR model. It is interesting to see that the QVAR model almost always outperforms the benchmark univariate specification, and that this better performance is statistically significant at the

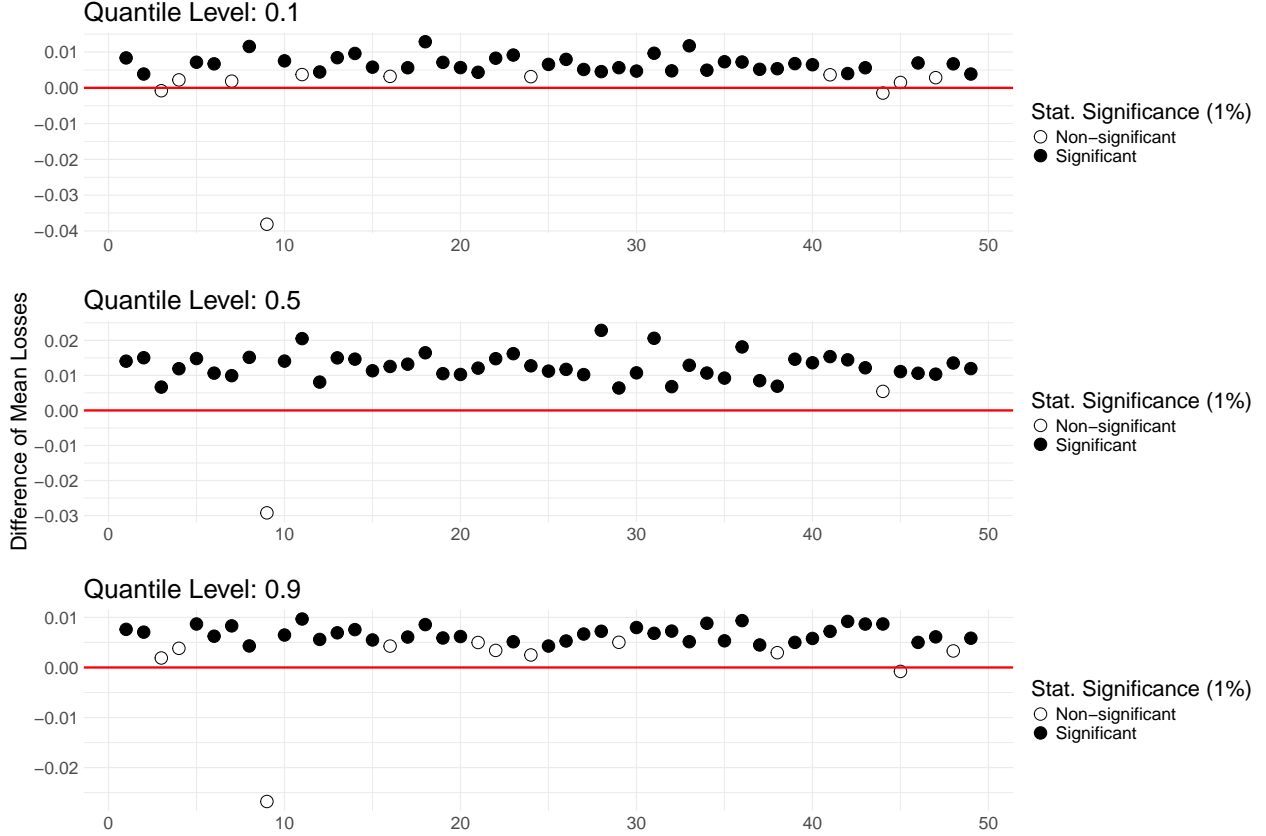


Figure (5) $\left(\tilde{\mathcal{L}}_{i,\tau} - \bar{\mathcal{L}}_{i,\tau}\right)$ values for $i = 1, \dots, 50$ and $\tau \in \{0.1, 0.5, 0.9\}$. *Notes:* $\tilde{\mathcal{L}}_{i,\tau}$ and $\bar{\mathcal{L}}_{i,\tau}$ are the average losses provided by the univariate QAR and LASSO-regularized QVAR models, respectively; a given point is full if the performance of the LASSO-regularized QVAR model is significantly better at the 1% significance level according to the Diebold and Mariano's (2002) test, and empty otherwise.

1% level in most cases. These findings highlight the importance of accounting for cross-sectional dependencies when modeling volatility in cryptocurrency markets. The superior predictive performance of the LASSO-regularized QVAR indicates that regularization is not only useful for addressing high dimensionality, but also crucial for capturing systemic interactions that drive forecasting accuracy. This has practical implications for both investors and risk managers, as more accurate forecasts of volatility quantiles can improve portfolio allocation and stress-testing exercises in an environment where traditional models often fail to capture tail dynamics.

6 Conclusions

The volatility interdependence of cryptocurrencies has been the subject of various empirical studies, but generally exhibit shortcoming in addressing the nonlinearities and heterogeneities inherent in the system of cryptocurrencies. In this paper, we extend the existing literature by modelling the spillover effect across a network of 50 major cryptocurrencies. Building on the quantile-based approach of connectedness (Ando et al., 2022) and following (Caporin et al., 2023), we employ a LASSO-regularized Quantile VAR framework. Interestingly, the LASSO regularization technique (Tibshirani, 1996) enhances the model’s predictive accuracy and sparsity, addressing the curse of dimensionality. As for the Quantile VAR approach of connectedness, it allows to capture the transmission of volatility shocks across various states, representing low, moderate, and high volatility states.

Using daily data from 50 cryptocurrencies over the period from August 8, 2015 to May 5, 2024, the following results emerge from our analysis. Firstly, based on the full-sample data, the spillover effect in high, medium, and low volatility regimes differs, although with a small magnitude. In this case, given the relatively large time dimension compared to the cross-sectional dimension ($T \gg N$), the role of LASSO regularization is less critical. Moreover, the estimated network appears relatively dense, as evidenced by the high values of the spillover indices over τ , a result that is corroborated by the alternative FNETS (Barigozzi et al., 2023) methodology. While FNETS does not allow for an extension of the analysis to different quantiles of the conditional distribution of volatilities, it has the advantage of filtering out common factors and isolating idiosyncratic connections, thereby providing a complementary perspective on the structure of volatility spillovers. In contrast, when moving to the rolling-window analysis, the dynamics across quantiles appear more heterogeneous, with larger differences emerging especially during tail events such as the COVID-19 pandemic and the war in Ukraine. In this setting, based on subsamples characterized by a lower T/N ratio, the role of LASSO regularization becomes more prominent, as dimensionality concerns are more binding and penalization proves crucial for stabilizing the estimates

and capturing the evolving structure of volatility spillovers. Secondly, our analysis highlights that systemic influence extends beyond the two dominant cryptocurrencies, Bitcoin and Ethereum. Several medium-sized cryptocurrencies also emerge as relevant transmitters of volatility, suggesting that contagion channels in the market are more dispersed than often assumed. Consequently, risk monitoring or regulatory oversight that concentrates exclusively on the largest cryptocurrencies could underestimate the breadth of systemic vulnerabilities in the crypto ecosystem. Thirdly, the forecasting exercise shows that the LASSO-regularized QVAR consistently outperforms its univariate counterpart across quantiles. The forecasting gains are statistically significant in most cases, underscoring the importance of accounting for cross-sectional dependencies and systemic interactions when predicting volatility in cryptocurrency markets. This result highlights that interconnectedness is not only a descriptive feature but also a source of predictive power.

Overall, our analysis provides a reasonable resolution to the high-dimensionality issues often faced by portfolio managers when dealing with a large set of cryptocurrencies. It demonstrates the utility of integrating the quantile-spillover approach with the LASSO technique to refine the spillover analysis across various levels of volatility and to deliver more accurate volatility forecasts. This has direct implications for investors, portfolio managers, and risk managers, while also being of interest to regulators and policymakers concerned with the development of this digital asset class. **In this regard, future research could extend our approach to include both cryptocurrencies and conventional assets, to better understand potential instability risk spillovers from cryptocurrencies to the global financial system.**

References

Aharon, D.Y., Demir, E., Lau, C.K.M., Zaremba, A., 2022. Twitter-based uncertainty and cryptocurrency returns. *Research in International Business and Finance* 59, 101546. doi:10.1016/j.ribaf.2021.101546.

- Ahn, Y., Kim, D., 2021. Emotional trading in the cryptocurrency market. *Finance Research Letters* 42, 101912. doi:10.1016/j.fr1.2020.101912.
- Anamika, Chakraborty, M., Subramaniam, S., 2023. Does sentiment impact cryptocurrency? *Journal of Behavioral Finance* 24, 202–218. doi:10.1080/15427560.2021.1950723.
- Ando, T., Greenwood-Nimmo, M., Shin, Y., 2022. Quantile connectedness: modeling tail behavior in the topology of financial networks. *Management Science* 68, 2401–2431. doi:10.1287/mnsc.2021.3984.
- Antonakakis, N., Chatziantoniou, I., Gabauer, D., 2019. Cryptocurrency market contagion: market uncertainty, market complexity, and dynamic portfolios. *Journal of International Financial Markets, Institutions and Money* 61, 37–51. doi:10.1016/j.intfin.2019.02.003.
- Barigozzi, M., Cho, H., Owens, D., 2023. FNETS: factor-adjusted network estimation and forecasting for high-dimensional time series. *Journal of Business & Economic Statistics* 42, 890–902. doi:10.1080/07350015.2023.2257270.
- Baur, D.G., Dimpfl, T., 2018. Asymmetric volatility in cryptocurrencies. *Economics Letters* 173, 148–151. doi:10.1016/j.econlet.2018.10.008.
- Belloni, A., Chernozhukov, V., 2011. ℓ_1 -penalized quantile regression in high-dimensional sparse models. *The Annals of Statistics* 39. doi:10.1214/10-aos827.
- Bonaccolto, G., Caporin, M., Gupta, R., 2018. The dynamic impact of uncertainty in causing and forecasting the distribution of oil returns and risk. *Physica A: Statistical Mechanics and its Applications* 507, 446–469. doi:10.1016/j.physa.2018.05.061.
- Bouri, E., Gupta, R., Roubaud, D., 2019a. Herding behaviour in cryptocurrencies. *Finance Research Letters* 29, 216–221. doi:10.1016/j.fr1.2018.07.008.

- Bouri, E., Molnár, P., Azzi, G., Roubaud, D., Hagfors, L.I., 2017. On the hedge and safe haven properties of Bitcoin: is it really more than a diversifier? *Finance Research Letters* 20, 192–198. doi:10.1016/j.fr1.2016.09.025.
- Bouri, E., Saeed, T., Vo, X.V., Roubaud, D., 2021. Quantile connectedness in the cryptocurrency market. *Journal of International Financial Markets, Institutions and Money* 71, 101302. doi:10.1016/j.intfin.2021.101302.
- Bouri, E., Shahzad, S.J.H., Roubaud, D., 2019b. Co-explosivity in the cryptocurrency market. *Finance Research Letters* 29, 178–183. doi:10.1016/j.fr1.2018.07.005.
- Brownlees, C.T., Gallo, G.M., 2009. Comparison of volatility measures: a risk management perspective. *Journal of Financial Econometrics* 8, 29–56. doi:10.1093/jjfinec/nbp009.
- Caporin, M., Bonaccolto, G., Shahzad, S.J.H., 2023. (Quantile) spillover indexes: simulation-based evidence, confidence intervals and a decomposition. *SSRN Electronic Journal* doi:10.2139/ssrn.4629224.
- Chowdhury, M.A.F., Abdullah, M., Alam, M., Abedin, M.Z., Shi, B., 2023. NFTs, DeFi, and other assets efficiency and volatility dynamics: an asymmetric multifractality analysis. *International Review of Financial Analysis* 87, 102642. doi:10.1016/j.irfa.2023.102642.
- Diebold, F.X., Mariano, R.S., 2002. Comparing predictive accuracy. *Journal of Business & Economic Statistics* 20, 134–144. doi:10.1198/073500102753410444.
- Diebold, F.X., Yilmaz, K., 2008. Measuring financial asset return and volatility spillovers, with application to global equity markets. *The Economic Journal* 119, 158–171. doi:10.1111/j.1468-0297.2008.02208.x.
- Diebold, F.X., Yilmaz, K., 2012. Better to give than to receive: predictive directional measurement of volatility spillovers. *International Journal of Forecasting* 28, 57–66. doi:10.1016/j.ijforecast.2011.02.006.

- Diebold, F.X., Yilmaz, K., 2014. On the network topology of variance decompositions: measuring the connectedness of financial firms. *Journal of Econometrics* 182, 119–134. doi:10.1016/j.jeconom.2014.04.012.
- Fasanya, I.O., Oyewole, O., Odudu, T., 2021. Returns and volatility spillovers among cryptocurrency portfolios. *International Journal of Managerial Finance* 17, 327–341. doi:10.1108/ijmf-02-2019-0074.
- Forni, M., Hallin, M., Lippi, M., Reichlin, L., 2000. The generalized dynamic-factor model: identification and estimation. *Review of Economics and Statistics* 82, 540–554. doi:10.1162/003465300559037.
- Granger, C.W.J., 1969. Investigating causal relations by econometric models and cross-spectral methods. *Econometrica* 37, 424. doi:10.2307/1912791.
- Gross, C., Siklos, P.L., 2019. Analyzing credit risk transmission to the nonfinancial sector in Europe: a network approach. *Journal of Applied Econometrics* 35, 61–81. doi:10.1002/jae.2726.
- Gurdgiev, C., O’Loughlin, D., 2020. Herding and anchoring in cryptocurrency markets: investor reaction to fear and uncertainty. *Journal of Behavioral and Experimental Finance* 25, 100271. doi:10.1016/j.jbef.2020.100271.
- Ji, Q., Bouri, E., Lau, C.K.M., Roubaud, D., 2019. Dynamic connectedness and integration in cryptocurrency markets. *International Review of Financial Analysis* 63, 257–272. doi:10.1016/j.irfa.2018.12.002.
- Karim, S., Lucey, B.M., Naeem, M.A., Uddin, G.S., 2022. Examining the interrelatedness of NFTs, DeFi tokens and cryptocurrencies. *Finance Research Letters* 47, 102696. doi:10.1016/j.fr1.2022.102696.

- Katsiampa, P., Corbet, S., Lucey, B., 2019. Volatility spillover effects in leading cryptocurrencies: a BEKK-MGARCH analysis. *Finance Research Letters* 29, 68–74. doi:10.1016/j.fr1.2019.03.009.
- Koenker, R., 2005. *Quantile Regression*. Cambridge University Press. doi:10.1017/cbo9780511754098.
- Koenker, R., Bassett, G., 1978. Regression quantiles. *Econometrica* 46, 33. doi:10.2307/1913643.
- Koutmos, D., 2018. Return and volatility spillovers among cryptocurrencies. *Economics Letters* 173, 122–127. doi:10.1016/j.econlet.2018.10.004.
- Kumar, A., Iqbal, N., Mitra, S.K., Kristoufek, L., Bouri, E., 2022. Connectedness among major cryptocurrencies in standard times and during the COVID-19 outbreak. *Journal of International Financial Markets, Institutions and Money* 77, 101523. doi:10.1016/j.intfin.2022.101523.
- Kumar, A.S., Anandarao, S., 2019. Volatility spillover in crypto-currency markets: some evidences from GARCH and wavelet analysis. *Physica A: Statistical Mechanics and its Applications* 524, 448–458. doi:10.1016/j.physa.2019.04.154.
- Kumar, S., Patel, R., Iqbal, N., Gubareva, M., 2023. Interconnectivity among cryptocurrencies, NFTs, and DeFi: evidence from the Russia-Ukraine conflict. *The North American Journal of Economics and Finance* 68, 101983. doi:10.1016/j.najef.2023.101983.
- Liu, J., Serletis, A., 2019. Volatility in the cryptocurrency market. *Open Economies Review* 30, 779–811. doi:10.1007/s11079-019-09547-5.
- Liu, J., Serletis, A., 2024. Volatility and dependence in cryptocurrency and financial markets: a copula approach. *Studies in Nonlinear Dynamics & Econometrics* 28, 119–149. doi:10.1515/snde-2022-0029.

- Liu, J., Zhou, Q., Lin, J., Hao, X., Chen, Z., 2025. Can real-time asymmetry and extreme dependence enhance the effectiveness of risk optimization in the cryptocurrency market? new evidence from the Mean-ES risk optimization framework based on the SHARV-MA-DMC model. *Applied Economics* , 1–17doi:10.1080/00036846.2025.2503488.
- Lütkepohl, H., 2005. *New introduction to multiple time series analysis*. Springer Berlin Heidelberg. doi:10.1007/978-3-540-27752-1.
- Maghyreh, A., Ziadat, S.A., 2024. Pattern and determinants of tail-risk transmission between cryptocurrency markets: new evidence from recent crisis episodes. *Financial Innovation* 10. doi:10.1186/s40854-023-00592-1.
- Mensi, W., El Khoury, R., Ali, S.R.M., Vo, X.V., Kang, S.H., 2023. Quantile dependencies and connectedness between the gold and cryptocurrency markets: effects of the COVID-19 crisis. *Research in International Business and Finance* 65, 101929. doi:10.1016/j.ribaf.2023.101929.
- Mokni, K., Bouteska, A., Nakhli, M.S., 2022. Investor sentiment and Bitcoin relationship: a quantile-based analysis. *The North American Journal of Economics and Finance* 60, 101657. doi:10.1016/j.najef.2022.101657.
- Pesaran, H., Shin, Y., 1998. Generalized impulse response analysis in linear multivariate models. *Economics Letters* 58, 17–29. doi:10.1016/s0165-1765(97)00214-0.
- Philippas, D., Rjiba, H., Guesmi, K., Goutte, S., 2019. Media attention and Bitcoin prices. *Finance Research Letters* 30, 37–43. doi:10.1016/j.fr1.2019.03.031.
- Shahzad, S.J.H., Bouri, E., Roubaud, D., Kristoufek, L., Lucey, B., 2019. Is Bitcoin a better safe-haven investment than gold and commodities? *International Review of Financial Analysis* 63, 322–330. doi:10.1016/j.irfa.2019.01.002.

- Tibshirani, R., 1996. Regression shrinkage and selection via the lasso. *Journal of the Royal Statistical Society: Series B (Methodological)* 58, 267–288. doi:10.1111/j.2517-6161.1996.tb02080.x.
- Xu, Q., Zhang, Y., Zhang, Z., 2021. Tail-risk spillovers in cryptocurrency markets. *Finance Research Letters* 38, 101453. doi:10.1016/j.fr1.2020.101453.
- Yi, S., Xu, Z., Wang, G.J., 2018. Volatility connectedness in the cryptocurrency market: is Bitcoin a dominant cryptocurrency? *International Review of Financial Analysis* 60, 98–114. doi:10.1016/j.irfa.2018.08.012.
- Yousaf, I., Yarovaya, L., 2022. Herding behavior in conventional cryptocurrency market, non-fungible tokens, and DeFi assets. *Finance Research Letters* 50, 103299. doi:10.1016/j.fr1.2022.103299.
- Zhang, L., Bouri, E., Chen, Y., 2023. Co-jump dynamicity in the cryptocurrency market: a network modelling perspective. *Finance Research Letters* 58, 104372. doi:10.1016/j.fr1.2023.104372.
- Özdemir, O., 2022. Cue the volatility spillover in the cryptocurrency markets during the COVID-19 pandemic: evidence from DCC-GARCH and wavelet analysis. *Financial Innovation* 8. doi:10.1186/s40854-021-00319-0.

A Supplementary material

Table (A1) Details on the selected cryptocurrencies

Name	Symbol	Daily Trading Volume (\$)	Market Cap (\$)
Bitcoin	BTC	18,296,164,805	1,261,203,911,122
Litecoin	LTC	266,211,647	6,062,317,973
XRP	XRP	535,784,827	29,263,355,596

Table A1 – continued from previous page

Name	Symbol	Daily Trading Volume (\$)	Market Cap (\$)
Dogecoin	DOGE	1,506,950,274	23,221,033,413
DigiByte	DGB	6,553,701	193,552,927
Dash	DASH	34,684,888	344,006,424
Monero	XMR	68,420,933	2,477,693,604
Stellar	XLM	44,733,799	3,210,014,206
Syscoin	SYS	2,141,955	158,767,615
Tether USDt	USDT	36,224,596,673	110,937,481,132
NEM	XEM	5,223,390	353,894,412
Ethereum	ETH	8,783,447,639	376,807,893,130
Siacoin	SC	11,705,945	417,141,043
Decred	DCR	2,879,041	345,822,923
Lisk	LSK	26,841,814	246,299,789
Waves	WAVES	31,517,294	279,091,701
Ethereum Classic	ETC	164,557,962	4,066,499,041
Neo	NEO	58,277,745	1,179,172,223
Zcash	ZEC	41,886,231	377,079,289
Golem	GLM	414,828,534	620,929,941
Maker	MKR	55,052,366	2,696,323,822
Nano	XNO	2,725,204	166,796,667
Ark	ARK	6,514,581	149,457,695
iExec RLC	RLC	10,592,925	204,657,881
Gnosis	GNO	13,691,713	820,180,845
Aragon	ANT	3,608,826	344,076,022
Qtum	QTUM	41,448,360	394,440,973
Basic Attention Token	BAT	13,206,967	371,484,136
IOTA	IOTA	11,831,147	740,921,434
Numeraire	NMR	9,768,560	167,354,130
Status	SNT	3,621,922	159,516,126
EOS	EOS	78,353,096	925,749,664
Storj	STORJ	9,987,280	225,301,992

Table A1 – continued from previous page

Name	Symbol	Daily Trading Volume (\$)	Market Cap (\$)
Gas	GAS	13,921,461	336,891,036
Civic	CVC	14,312,549	167,076,684
Bitcoin Cash	BCH	231,293,769	9,245,270,871
BNB	BNB	531,182,053	87,392,373,029
0x Protocol	ZRX	15,806,355	426,904,271
Loopring	LRC	10,746,141	356,723,857
TRON	TRX	196,753,191	10,599,560,420
Decentraland	MANA	35,024,089	854,461,527
Propy	PRO	6,129,584	292,154,972
Chainlink	LINK	190,221,873	8,439,845,145
Cardano	ADA	239,700,527	16,340,709,993
Tezos	XTZ	19,767,609	946,265,354
Bitcoin Gold	BTG	79,871,514	670,318,809
KuCoin Token	KCS	1,268,257	990,310,834
ICON	ICX	3,373,217	227,762,038
Enjin Coin	ENJ	14,043,906	425,368,437
Powerledger	POWR	8,892,225	156,672,625

Notes: This table provides details on the 50 selected cryptocurrencies as of May 5, 2024.